

DMD#84897

Title page

**Pharmacokinetics, Metabolism, and Excretion of [¹⁴C]Esaxerenone, a Novel Mineralocorticoid
Receptor Blocker in Humans**

Makiko Yamada, Jeanne Mendell, Hideo Takakusa, Takako Shimizu, Osamu Ando

Drug Metabolism and Pharmacokinetics Research Laboratories (M.Y., H.S., O.A.) and Clinical

Pharmacology Department (T.S.), Daiichi Sankyo Co., Ltd., Tokyo, Japan; and Daiichi Sankyo Pharma

Development, Basking Ridge, NJ, USA (J.M.)

DMD#84897

Running title page

Running title: Esaxerenone ADME in Humans and In Vitro

*Corresponding author: Makiko Yamada, Drug Metabolism and Pharmacokinetics Research Laboratories,

Daiichi Sankyo Co., Ltd., 1-2-58, Hiromachi, Shinagawa-ku, Tokyo 140-8710, Japan. Phone:

+81-3-3492-3131; Fax: +81-3-5436-8567. E-mail: yamada.makiko.jr@daiichisankyo.co.jp

Number of text pages: 25

Number of tables: 3

Number of figures: 7

Number of references: 27

Number of words in the Abstract: 250

Number of words in the Introduction: 747

Number of words in the Discussion: 1494

Abbreviations: AUC, area under the blood or plasma concentration-time curve; BCRP, breast cancer resistance protein; CL_t, total body clearance; CL/F, apparent total body clearance; CYP, cytochrome P450; DDI, drug-drug interaction; LC-MS/MS, liquid chromatography-tandem mass spectrometry; HPLC, high-performance liquid chromatography; P450, cytochrome P450; P-gp, P-glycoprotein; t_{1/2}, elimination half-life in the terminal phase; T_{max}, time to reach the maximum plasma concentration; UGT, UDP-glucuronosyltransferase; and V_z/F, apparent volume of distribution based on the terminal phase.

DMD#84897

Abstract

Esaxerenone (CS-3150) is a novel, non-steroidal, selective mineralocorticoid receptor blocker. The absorption, metabolism, distribution, and excretion (ADME) of esaxerenone were assessed in in vitro studies and in a clinical study, where [^{14}C]esaxerenone (150 μCi /20 mg) was administered orally to six healthy male subjects. The plasma concentrations of esaxerenone and its metabolites, M4, M11, and M1, were measured using LC-MS/MS. The recovery of radioactivity was 92.5%, with 38.5% and 54.0% excreted in the urine and feces, respectively. The half-life of radioactivity in blood and plasma was approximately 30 h, similar to that of the unchanged form in plasma. The blood-to-plasma ratio was 0.69, demonstrating low partitioning to blood components. In plasma, esaxerenone was the most abundant moiety (40.8%), followed by O-glucuronide (21.4%; M4), acyl-glucuronide of amide-bond hydrolysate (8.0%; M11) and the deshydroxyethyl form (1.7%; M1). In vitro studies showed that esaxerenone was a substrate of CYP3A and multiple UGT isoforms. Oxidation contributed approximately 30% to its clearance, as indicated by the excretion ratio of oxidized metabolites into urine and feces. Caco-2 studies showed that esaxerenone was a substrate of P-gp and BCRP; however, the excretion ratio of the unchanged form in the feces and urine was 18.5% and 1.6%, respectively, indicating that these transporters were not important for the absorption and elimination of esaxerenone. Low urinary excretion of esaxerenone suggested that the plasma exposure of esaxerenone was not affected by renal dysfunction. Multiple elimination pathways, including oxidation, glucuronidation, and hydrolysis, and the low contribution of transporters, indicated limited drug-drug interaction potential.

Introduction

Mineralocorticoid receptors (MR) that are present in the epithelial cells of the distal tubule and collecting duct in the kidney have been reported to play a role in the regulation of electrolyte homeostasis, body fluids, and blood pressure via activation by aldosterone (Funder, 1996). In addition, MRs have been reported to be expressed in non-epithelial tissues such as podocytes (Shibata *et al.*, 2007), mesangial cells (Nishiyama *et al.*,

DMD#84897

2005), fibroblasts (Nagai *et al.*, 2005), and the heart (Lombès *et al.*, 1995). Excessive MR activation by endogenous ligands (e.g., aldosterone) is involved in the pathogenesis of renal disorders, which may be caused by direct enhancement of fibrosis (Brem *et al.*, 2011), inflammation (Siragy and Xue, 2008), and oxidative stress (Patni *et al.*, 2007). Multiple clinical studies using steroidal MR blockers, such as spironolactone and eplerenone, have shown that MR blockade is a favorable strategy for the treatment of hypertension (Saruta *et al.*, 2004), heart failure (Pitt *et al.*, 1999, 2003), and chronic kidney disease (Rossing *et al.*, 2005; Epstein *et al.*, 2006). However, the clinical use of existing MR antagonists is limited by their safety and efficacy profiles (Rose *et al.*, 1977; Weinberger *et al.*, 2002).

Esaxerenone (CS-3150) is a novel, non-steroidal, selective MR blocker. An *in vitro* study showed that esaxerenone inhibited the binding of aldosterone to the MR, with no agonistic or antagonistic effects on glucocorticoid, androgen, or progesterone receptors, even at high concentrations (Arai *et al.*, 2015a). In pharmacology studies using rat models, esaxerenone was demonstrated to have potent and long-lasting antihypertensive and cardio-renal protective effects (Arai *et al.*, 2015a; Arai *et al.*, 2015b; Arai *et al.*, 2016). In clinical studies, esaxerenone dose-dependently reduced blood pressure in patients with hypertension (submitted for publication); further, the reduction of urinary albumin in patients with type 2 diabetes with microalbuminuria underscores its renal protective effects (submitted for publication). In pharmacokinetic studies, the absolute oral bioavailability of esaxerenone was high in rats and monkeys (Yamada *et al.*, 2017). The half-life ($t_{1/2}$) of esaxerenone in plasma is longer than that of spironolactone and eplerenone in rats, and is considered to contribute to its long-lasting pharmacological effects. In rats, orally administered [^{14}C]esaxerenone was distributed widely to tissues, with the exception of a low distribution to the central nervous system (Yamada *et al.*, 2017). After the oral administration of [^{14}C]esaxerenone, the major elimination pathway was oxidation in rats, and oxidation and glucuronidation in monkeys, and the radioactivity was excreted mainly in the feces (Yamada *et al.*, 2017). In Phase 1 studies, the exposure of esaxerenone after single (5 to 200 mg/day) and multiple (10 to 100 mg/day) doses was generally proportional to the dose (Kato *et al.*,

DMD#84897

2018). The time to reach the maximum plasma concentration (T_{\max}) and $t_{1/2}$ after single oral administration were approximately 3 h and 20 h, respectively, and did not change across dose levels (Kato *et al.*, 2018). The $t_{1/2}$ appears to be suitable for once-daily dosing because efficacy is expected to be sustained throughout the day. The total apparent clearance of drug and apparent volume of distribution also remained constant, regardless of dose. The exposure to esaxerenone in the multiple-dose treatment was greater on Day 10 than on Day 1, and the accumulation ratio was in the range 1.36–1.98 (Kato *et al.*, 2018).

Absorption, distribution, metabolism, and excretion (ADME) studies are an essential part of drug development as the ADME properties of a drug candidate are associated with its efficacy and safety. The use of radioactive tracers in ADME studies, such as ^{14}C -labeled compounds, enables us to determine the major metabolic and excretory routes of elimination of a drug candidate. Such information is necessary to determine the drug-drug interaction (DDI) potential and the influence of renal or hepatic dysfunction. The guidance on metabolites in safety testing (MIST guidance) from the Food and Drug Administration (FDA) states that the exposure of metabolites should be determined to evaluate the necessity of additional safety assessment of metabolites (FDA, 2016). Owing to the evolution of analytical techniques, in most cases, metabolites in plasma can be detected without using labeled compounds. However, to prove that no metabolite that requires evaluation has been overlooked, studies using radiolabeled compounds are still necessary. In this study, [^{14}C]esaxerenone was administered to healthy male subjects and the pharmacokinetics, metabolism, and excretion were evaluated. In addition, the enzymes involved in the metabolism, cytochrome P450 (P450) and UDP-glucuronosyltransferase (UGT), and the transporters involved in the absorption of esaxerenone, P-glycoprotein (P-gp) and breast cancer resistance protein (BCRP), were evaluated.

Materials and Methods

Compounds and Reagents

[^{14}C]esaxerenone,

DMD#84897

(5*P*)-1-(2-hydroxyethyl)-*N*-[4-(methanesulfonyl)phenyl]-4-methyl-5-[2-(trifluoromethyl)phenyl]-[4-¹⁴C]-1*H*-pyrrole-3-carboxamide was supplied by ABC Laboratories Inc. (Columbia, MO); the structure is shown in Figure 1. Non-radiolabeled esaxerenone, ((*S*)-1-(2-hydroxyethyl)-4-methyl-*N*-[4-(methylsulfonyl)phenyl]-5-[2-(trifluoromethyl)phenyl]-1*H*-pyrrole-3-carboxamide) and deuterium-labeled esaxerenone (Figure 1) were synthesized at Daiichi Sankyo (Tokyo, Japan). The metabolites of esaxerenone, 4-methyl-*N*-[4-(methylsulfonyl)phenyl]-5-[2-(trifluoromethyl)phenyl]-1*H*-pyrrole-3-carboxamide (M1), (*S*)-(3-methyl-4-{[4-(methylsulfonyl)phenyl]carbamoyl}-2-[2-(trifluoromethyl)phenyl]-1*H*-pyrrol-1-yl)acetic acid (M2), (*S*)-1-(2-hydroxyethyl)-4-(hydroxymethyl)-*N*-[4-(methylsulfonyl)phenyl]-5-[2-(trifluoromethyl)phenyl]-1*H*-pyrrole-3-carboxamide (M3), 2-[(*S*)-(3-methyl-4-{[4-(methylsulfonyl)phenyl]carbamoyl}-2-[2-(trifluoromethyl)phenyl]-1*H*-pyrrol-1-yl)]ethyl β-D-glucopyranosiduronic acid (M4), ((*S*)-3-(hydroxymethyl)-4-{[4-(methylsulfonyl)phenyl]carbamoyl}-2-[2-(trifluoromethyl)phenyl]-1*H*-pyrrol-1-yl)acetic acid (M5), and deuterium-labeled M1 were also synthesized at Daiichi Sankyo. The metabolite M11, 1-*O*-({(5*P*)-1-(2-hydroxyethyl)-4-methyl-5-[2-(trifluoromethyl)phenyl]-1*H*-pyrrol-3-yl}carbonyl)-β-D-glucopyranuronic acid was synthesized at Daiichi Sankyo RD Novare (Tokyo, Japan). [¹⁴C]4-(methylsulfonyl)aniline (4MSA), a metabolite generated by the hydrolysis of esaxerenone, was synthesized at Curachem, Inc. (Chungcheongbuk, Korea). Esaxerenone and M1 were synthesized by using the method described in the patent applications (Canne Bannen *et al.*, 2006; Aoki *et al.*, 2008). M2 and M3 were prepared in a similar manner as that mentioned in the patent applications described above. M4 was synthesized via conventional *O*-glycosidation of the alcohol in esaxerenone, followed by the removal of the protective group. M11 was prepared biosynthetically by using microorganisms from 1-(2-Hydroxyethyl)-4-methyl-5-[2-(trifluoromethyl)phenyl]-1*H*-pyrrole-3-carboxylic acid (HMCA). Microsomes from baculovirus-infected insect cells expressing human P450 or UGT isoforms were purchased

DMD#84897

from BD Biosciences (San Jose, CA) and Corning (Corning, NY). A Reaction Phenotyping Kit (version 8) containing human liver microsomes from 16 individual donors was purchased from XenoTech (Kansas City, KS). NADPH regeneration system solution A, NADPH regeneration system solution B, UGT reaction mix solution A, and UGT reaction mix solution B were purchased from Corning Inc. Caco-2 cells were obtained from American Type Culture Collection (Manassas, VA). [^3H]Digoxin, [^3H]estrone sulfate ammonium salt, and [^{14}C]mannitol were purchased from PerkinElmer (Waltham, MA). [^{14}C]Theophylline was purchased from American Radiolabeled Chemicals (St. Louis, MO). Verapamil hydrochloride and novobiocin sodium salt were purchased from Sigma-Aldrich (St. Louis, MO). GF120918 was purchased from Toronto Research Chemicals (North York, Canada). Antibiotic-antimycotic (100 \times) liquid, L-glutamine-200 mM liquid, Dulbecco's modified Eagle's medium (DMEM), fetal bovine serum (FBS), and 10 \times Hanks' balanced salt solution (HBSS) were purchased from Thermo Fisher Scientific (Waltham, MA). Other reagents were commercially available and of special reagent grade, HPLC grade, LC-MS grade, or equivalent.

Clinical Study Design and Sample Collection

The study was conducted at Worldwide Clinical Trials (San Antonio, TX) in six healthy male subjects between 18 and 60 years of age. The study was conducted in compliance with ethical principles that have their origin in the Declaration of Helsinki and was approved by the institutional review board (IntegReview) on August 26, 2015. All participants provided written informed consent prior to commencement of the study. Each of the six subjects received a single oral dose of [^{14}C]esaxerenone (150 μCi /20 mg) as a solution after fasting for at least 8 h. Subjects continued to fast for an additional 4 h after dosing. Whole blood and plasma samples were collected at the following times: 0 (pre-dose), 0.5, 1, 1.5, 2, 2.5, 3, 3.5, 4, 6, 8, 12, 16, 24, 36, 48, 60, 72, 96, 120, 132, 144, 156, 168, 180, 192, 216, 240, 264, and 288 h post dose. Urine samples were collected over the following intervals: -2 to 0 h (pre-dose), 0 to 4, 4 to 8, 8 to 12, 12 to 24, 24 to 36, 36 to 48, 48 to 72, 72 to 96, 96 to 120, 120 to 144, 144 to 168, 168 to 192, 192 to 216, 216 to 240, 240 to 264, and 264 to 288 h post dose.

DMD#84897

The fecal samples were collected at the following times: 0, 0 to 24, 24 to 48, 48 to 72, 72 to 96, 96 to 120, 120 to 144, 144 to 168, 168 to 192, 192 to 216, 216 to 240, 240 to 264, and 264 to 288 h post dose; mixed with water, and homogenized. The samples were stored at approximately -80°C until analysis.

Analysis of Total Radioactivity, Esaxerenone, and Metabolite Concentration

The total radioactivity in blood, plasma, urine, and feces was measured by using a liquid scintillation counter (LSC) at Worldwide Clinical Trials. Plasma esaxerenone and metabolite concentrations were measured by a validated liquid chromatography-tandem mass spectrometry (LC-MS/MS) assay at Celerion (Lincoln, NE) using an electrospray ionization (ESI) interface in the positive ion mode. The detailed method of analysis is shown in the supplemental data (Supplemental Method).

Pharmacokinetic Analysis

Plasma concentration-time data for esaxerenone and metabolites, and total radioactivity concentration-time data for [^{14}C]esaxerenone equivalents in plasma and whole blood were analyzed by using non-compartmental methods in Phoenix WinNonlin (version 6.3, Pharsight Corporation, Mountain View, CA). The following parameters were calculated: area under the plasma concentration versus time curve up to the last measurable time point (AUC_{last}), area under the plasma concentration versus time curve to infinity (AUC_{inf}), maximum plasma concentration (C_{max}), time to reach the maximum plasma concentration (T_{max}), and elimination half-life at terminal phase ($t_{1/2}$). For esaxerenone, the apparent total body clearance (CL/F) and apparent volume of distribution based on the terminal phase (V_z/F) were also calculated. AUC_{inf} and $t_{1/2}$ were not calculated unless at least three time points (of which the first time point must be greater than T_{max}) with quantifiable concentrations were obtained. The blood-to-plasma AUC_{last} ratio was calculated by dividing AUC_{last} of total radioactivity in blood by AUC_{last} of total radioactivity in plasma. The AUC ratio of esaxerenone and metabolites to total radioactivity (AUCR , %) was calculated by dividing AUC_{inf} of

DMD#84897

esaxerenone or metabolite by AUC_{inf} of total radioactivity. AUC_{last} was used for M1 instead of AUC_{inf} because AUC_{inf} was not calculated for M1. When calculating AUCR, AUC was converted into the molar amounts using the molecular weights of 466.47 for esaxerenone, 422.42 for M1, 642.60 for M4, and 489.40 for M11; AUC for total radioactivity in molar amounts was determined by using the specific activity of [^{14}C]esaxerenone. The excretion of radioactivity in urine and feces (% of dose) was calculated by dividing excreted radioactivity by administered radioactivity.

Metabolite Profiling of Human Plasma, Urine, and Feces

The plasma samples collected at 1 h post dose were pooled by mixing an equal volume from each subject, and qualitatively analyzed. The pooled urine (0 to 24 h for qualitative analysis; and 0 to 24, 24 to 48, and 48 to 72 h for quantitative analysis) and feces (24 to 48 h for qualitative analysis; and 0 to 24, 24 to 48, 48 to 72, 72 to 96, and 96 to 168 h for quantitative analysis) samples were prepared by proportional mixing from each subject based on the amount, and combining a proportionally excreted amount from each time point, and then used for analysis. The plasma, urine, or fecal samples were extracted with acetonitrile and analyzed by using radio-HPLC and MS detector, qualitatively and quantitatively. The detailed analysis method is shown in the supplemental data (Supplemental Method). For the quantitative analysis, the percentage area of each radioactive peak on the radiochromatogram was calculated with analysis software (FLO-ONE, PerkinElmer). The excretion ratios of esaxerenone and metabolites in urine and feces were calculated by multiplying the total excretion ratios of radioactivity in the urine and feces (% of dose) by the composition ratio of each radioactive peak, and shown as a cumulative value.

In vitro Identification of P450 Isoform

Two studies were conducted to identify the P450 isoforms involved in the oxidative metabolism of esaxerenone. For the recombinant study, esaxerenone was incubated with the microsomes from

DMD#84897

baculovirus-infected insect cells expressing human cytochrome P450 (P450) isoforms (CYP1A2, CYP2B6, CYP2C8, CYP2C9, CYP2C19, CYP2D6, CYP3A4, and CYP3A5; final concentration: 30 pmol P450/mL). For the correlation analysis, esaxerenone was incubated with each individual type of human liver microsomes (final concentration: 1 mg protein/mL). The concentrations of M1, M2, and M3 were measured by using an LC-MS/MS method. The detailed method is shown in the supplemental data (Supplemental Method). The formation rates of the metabolites were calculated by dividing the concentration of the metabolites by the incubation time and the P450 (nmol P450/mL) or protein (mg protein/mL) concentration in microsomes. For the correlation analysis, the coefficient of determination (R^2) was calculated from the plot of each P450 isoform activity based on the specific marker reactions in individual human liver microsomes and the formation rates of the metabolites. The P450 isoform activities based on the specific marker reactions in individual human liver microsomes were cited from the data sheet provided by XenoTech, LLC.

In vitro UGT Isoform Identification

Esaxerenone was incubated with the microsomes from baculovirus-infected insect cells expressing human UDP-glucuronosyltransferase (UGT) isoforms (UGT1A1, UGT1A3, UGT1A4, UGT1A6, UGT1A9, UGT2B7, and UGT2B15; final concentration: 0.5 mg protein/mL), and the concentrations of M4 were measured by using an LC-MS/MS method. The detailed method is shown in the supplemental data (Supplemental Method). The formation rates of M4 were calculated by dividing the concentration of M4 by the incubation time and the protein concentration of the microsomes (mg protein/mL).

Transcellular Transport Across Caco-2 Cells via P-gp and BCRP

To evaluate the transcellular transport via P-gp and BCRP, Caco-2 cells were seeded at a density of 1×10^5 cells/cm² in 24 well plates. For the bidirectional transport assay, the medium at the apical side and basal side of the plate was removed by aspiration and replaced with HBSS or HBSS containing 100 μ M verapamil

DMD#84897

(typical P-gp inhibitor, Rautio *et al.*, 2006), 10 μ M novobiocin (typical BCRP inhibitor, Xia *et al.*, 2005), or 10 μ M GF120918 (P-gp and BCRP inhibitor, Xia *et al.*, 2005), and the plate was preincubated at 37°C for 1 h. After the preincubation, the solution in the donor side was replaced with HBSS buffer containing 1 μ M [14 C]esaxerenone (with or without inhibitors), 1 μ M [3 H]digoxin (typical P-gp substrate, with or without inhibitors), 0.1 μ M [3 H]estrone sulfate (typical BCRP substrate, with or without inhibitors), 10 μ M [14 C]theophylline (high-permeability marker), or 10 μ M [14 C]mannitol (low permeability marker). After incubation for a designated period at 37°C, the receiver side solution was collected into a glass vial. The assay solution (10 μ L) was collected from the donor side after 1 h and the radioactivity was counted by using LSC. Incubation was performed in triplicate. The detailed method is shown in the supplemental data (Supplemental Method).

The permeability coefficient (P_{app}) and the P_{app} ratio of the test compounds were calculated using the following equations:

$$P_{app} \text{ (cm/sec)} = [dQ/dt]/A/C_{donor}$$

where dQ/dt is the transport rate (dpm/sec), A is the surface area of the monolayer (cm^2), and C_{donor} is the observed concentration in donor sample collected after incubation for 1 h (dpm/mL).

$$P_{app} \text{ ratio} = P_{app, A \text{ to } B} / P_{app, B \text{ to } A}$$

where $P_{app, A \text{ to } B}$ is the P_{app} value from the apical-to-basal direction and $P_{app, B \text{ to } A}$ is the P_{app} value from the basal-to-apical direction.

Metabolism and Excretion of Esaxerenone Hydrolysate in Rats

In the course of the metabolite profiling, the hydrolysis of the central amide bond of esaxerenone was observed. Only methyl-(trifluoromethyl)phenyl-hydroxyethyl-pyrrole carboxylate side was radiolabeled and detected; however, the complementary part, 4-(methylsulfonyl)aniline (4MSA), must also be produced in the body. As the hydrolyzed metabolite was not observed in rats and monkeys, further non-clinical evaluation was

DMD#84897

difficult, even if another [^{14}C]esaxerenone with labeled 4MSA was synthesized. Therefore, [^{14}C]4MSA was synthesized to investigate its fate and administered intravenously to fasted male F344 rats (Charles River Laboratories Japan, Shiga, Japan) at 1 mg/kg. All animal experiments were conducted in accordance with the guidelines of the Institutional Animal Care and Use Committee of Daiichi Sankyo Co., Ltd. For the pharmacokinetic study (n=3), the blood was collected from the jugular vein at the designated sample collection times and the plasma was obtained by centrifugation. The concentration of radioactivity in blood and plasma was measured by LSC. For the mass balance study (n=3), the rats were housed individually in the glass metabolic cages (Metabolica, Sugiyama-Gen Iriki, Tokyo, Japan) after the drug administration, and the urine and feces were collected for the designated periods. The concentration of radioactivity in the urine and feces was measured by LSC and excretion ratio of radioactivity (% of dose) was calculated by dividing the excreted radioactivity by the administered radioactivity. For metabolite profiling, the blood was collected from the abdominal aorta at 1 and 6 h after administration and the plasma was obtained by centrifugation. The structure of metabolites was elucidated using LC-MS/MS coupled with a radioactivity detector. The detailed conditions of the analysis are shown in the supplemental data (Supplemental Figure 3).

Results

Pharmacokinetics and Excretion of [^{14}C]Esaxerenone

The radioactivity concentration-time profiles in blood and plasma after a single oral administration of 20 mg [^{14}C]esaxerenone to healthy volunteers are shown in Figure 2A, and the pharmacokinetic parameters for radioactivity are shown in Table 1. Mean C_{max} of radioactivity in plasma and blood was 430 and 281 ng-eq./mL respectively; mean AUC_{last} was 12,600 and 7880 ng-eq.·h/mL, and mean AUC_{inf} was 12,900 and 8180 ng-eq.·h/mL, respectively. Median T_{max} and mean $t_{1/2}$ were approximately 4 and 30 h both in blood and plasma, respectively. The blood-to-plasma AUC_{last} ratio of the radioactivity was 0.628. Mean plasma concentrations of esaxerenone and its metabolites are shown in Figure 2B. The pharmacokinetic parameters of

DMD#84897

esaxerenone and metabolites are presented in Table 1. The mean $t_{1/2}$ values of esaxerenone, M4, and M11 were 34.0, 27.8, and 26.4 h, respectively. The $t_{1/2}$ of M1 was not determined owing to its slow elimination; however, the exposure was very low. Mean C_{\max} was 237 ng/mL for esaxerenone, followed by 165 ng/mL (M4), 39.0 ng/mL (M11), and 1.00 ng/mL (M1). Mean exposure (AUC_{last} for M1 and AUC_{inf} for others) was 5320 ng·h/mL for esaxerenone, followed by 3860 ng·h/mL (M4), 1070 ng·h/mL (M11), and 198 ng·h/mL (M1), respectively. Based on AUC_{inf} total radioactivity ratios, esaxerenone was the most abundant moiety in plasma (40.8%), followed by M4 (21.4%) and M11 (8.0%). Based on AUC_{last} , the abundance of M1 was 1.7% of the total radioactivity. The total recovery of radioactivity in urine and feces over the 288 h sampling period was 92.5%, with 76.6% recovered by 96 h and 86.7% recovered by 144 h, as shown in Figure 3. The cumulative percentage of radioactivity recovered in urine and feces was 38.5% and 54.0%, respectively.

Structure Elucidation of Metabolites

Structural elucidation of the metabolites in plasma, urine, and feces collected after the oral administration of [^{14}C]esaxerenone was conducted by using LC-MS/MS combined with a radioactivity detector; representative radiochromatograms are shown in Figure 4. Structural assignment and mass spectrometry data were summarized in Table 2. The fragmentation schemes of esaxerenone and metabolites are shown in the supplemental data (Supplemental Figure 1).

Plasma

In plasma, unchanged esaxerenone was detected as the largest peak. Two radioactive peaks of the metabolites M4 and M11 were detected. M4 was identified to the *O*-glucuronide of esaxerenone, similar to that found in monkey plasma (Yamada *et al.*, 2017). The structure of M4 is shown in Figure 5. The deprotonated molecule $[\text{M}-\text{H}]^-$ ion of M11 was detected at m/z 488. One of the major product ions of M11 was detected at m/z 312, which corresponded to the loss of the glucuronic acid group (176 Da). The product ion at m/z 312 also

DMD#84897

corresponded to the methyl-(trifluoromethyl)phenyl-hydroxyethyl-pyrrole carboxylate, suggesting that M11 was a glucuronide of the esaxerenone amide-bond hydrolysate. By comparing the retention time and LC-MS/MS spectra with those of the authentic standard, M11 was identified as the acyl-glucuronide of esaxerenone amide-bond hydrolysate. M1, which was identified in rat plasma (Yamada *et al.*, 2017) was detected only by mass spectrometry and was not detected by radiochromatography.

Urine

In urine, the unchanged forms, M2, M3, M4, M5, M8, M11, M12, and M13 were detected. M2, M3, and M5 were also detected in rat and monkey samples (Yamada *et al.*, 2017), and identified as the carboxylic acid form in the *N*-alkyl side chain, the hydroxymethyl form of esaxerenone, and the hydroxymethyl form of M2 (or the carboxylic acid form of M3), respectively (Figure 5).

The deprotonated molecule $[M-H]^-$ ion of M8 and M13 was detected at m/z 657, which was 192 Da larger than the m/z 465 of esaxerenone. The mass shift from esaxerenone corresponded to $C_6H_8O_7$, which was attributable to the combination of monooxygenation (+O) and glucuronidation ($+C_6H_8O_6$). In addition, the major fragment ions at m/z 481 and 463 were attributable to the loss of the glucuronic acid moiety and its dehydration product. As the fragment ion at m/z 170 indicated no changes in the methylsulfonylphenyl group and the structure analysis of M3 demonstrated that the major oxidation site for esaxerenone was the methyl group on the pyrrole moiety as described below, M8 and M13 were proposed to be glucuronides of M3; however, the conjugated position has not yet been determined.

The deprotonated molecule $[M-H]^-$ ion of M12 was detected at m/z 488. In the same way as M11, one of the major product ions at m/z 312 corresponded to the loss of the glucuronic acid group (176 Da) from the glucuronide of the esaxerenone amide-bond hydrolysate. As M11 was identified to be the acyl-glucuronide by using an authentic standard, M12 was estimated to be an *O*-glucuronide of esaxerenone amide-bond hydrolysate.

DMD#84897

Feces

In feces, the unchanged forms, M2, M3, M5, M15, M16, and M17 were detected. The deprotonated molecule $[M-H]^-$ ion of M15 was detected at m/z 467, and its molecular composition was estimated to be $C_{21}H_{19}F_3N_2O_5S$ based on the accurate mass detected, which indicated that M15 was the demethylated ($-CH_2$) and monooxygenated ($+O$) form of esaxerenone. Together with mass fragmentation analysis, M15 was estimated as the sulfonic acid form of esaxerenone; assignment of the fragment ions is shown in Supplemental Figure 1.

At the elution times of M16 and M17, m/z 497 was detected in the mass spectrum, and its accurate mass corresponded to $C_{22}H_{21}F_3N_2O_6S$, indicating that M16 and M17 were the dioxygenated ($+2O$) forms of esaxerenone. The site of oxidation for M16 was not identified because the product ion scan data were not obtained owing to the low intensity of the precursor ion. In the case of M17, the fragment ion m/z values of 170, 300, and 351 were detected as key fragment ions in the CID/HCD product ion scan. From these data, the oxidation position for M17 was estimated to be on the pyrrole moiety containing the methyl and hydroxyethyl groups; assignment of the fragment ions is shown in Supplemental Figure 1.

Quantitative Metabolite Profiling

To assess the urinary and fecal excretion of the unchanged form and major metabolites, the urine collected from 0 to 72 h and the feces collected from 0 to 168 h were analyzed, and the results are shown in Table 3. After the oral administration of $[^{14}C]$ esaxerenone to humans, the excretion of unchanged esaxerenone in urine was only 1.6%. M11 was excreted in urine at 10.5% of the dose as a major metabolite, followed by M4 (7.2%). In feces, esaxerenone was excreted at 18.7% of the dose and the major metabolites excreted were M3 and M5 (10.1%, sum of both metabolites) and M2 (9%). The total excretion ratio of the oxidized metabolites (M2, M3, M5, M16, and M17) and the conjugated forms of the oxidized metabolites (M8 and M13) was 28.9%.

DMD#84897

P450 and UGT Isoform Identification

Esaxerenone was incubated with microsomes from baculovirus-infected insect cells expressing human CYP1A2, CYP2B6, CYP2C8, CYP2C19, CYP2D6, CYP3A4, and CYP3A5, and the production of the oxidized metabolites (M1, M2, and M3) was determined by LC-MS/MS. The results are shown in Figure 6A. The mean formation rates of M1, M2, and M3 in the microsomes expressing human P450 isoforms were 2.08, 2.06, and 136 pmol/min/nmol P450 for CYP3A4; and 0.647, 4.30, and 8.23 pmol/min/nmol P450 for CYP3A5, respectively. No metabolites were produced by other P450 isoforms. Esaxerenone was also incubated with human liver microsomes from 16 individual donors. The formation rates of metabolites by human liver microsomes were highly correlated with testosterone 6 β -hydroxylation and midazolam 1'-hydroxylation, which are markers of CYP3A4/5 activity, with correlation coefficients (r^2) of 0.813, 0.842, and 0.807 for M1, M2, and M3, respectively (testosterone 6 β -hydroxylation) and 0.707, 0.693, and 0.794, for M1, M2, and M3, respectively (midazolam 1'-hydroxylation). For the other P450 isoform activities, no apparent correlation was observed (Supplemental Figure 2). These results indicated that CYP3A4 and CYP3A5 were the main isoforms involved in the oxidative metabolism of esaxerenone by P450 in the human liver. For UGT isoform identification, esaxerenone was incubated with microsomes from baculovirus-infected insect cells expressing human UGT1A1, UGT1A3, UGT1A4, UGT1A6, UGT1A9, UGT2B7, and UGT2B15; subsequently, the production of its metabolite, M4, was determined by LC-MS/MS. The results are shown in Figure 6B. The formation rates of M4 for UGT1A1, UGT1A3, UGT1A4, UGT1A9, UGT2B7, and UGT2B15 were 0.932, 0.289, 0.115, 0.182, 0.837, and 0.668 pmol/min/mg protein, respectively. These results indicated that multiple UGT isoforms were involved in the *O*-glucuronidation of esaxerenone.

Transcellular Transport Across Caco-2 Cell Via P-gp and BCRP

The transcellular transport of [14 C]esaxerenone and the effects of P-gp and BCRP inhibitors investigated using

DMD#84897

Caco-2 cell monolayers are shown in Figure 7. The electrical resistance was between 0.468 and 0.510 kΩ·cm². The P-gp and BCRP activities in Caco-2 cell monolayers were confirmed by vectorial transport of [³H]digoxin (a P-gp substrate) and [³H]estrone sulfate (a BCRP substrate), which was inhibited in the presence of verapamil (a P-gp inhibitor) and novobiocin (a BCRP inhibitor), respectively (Figure 7A). The vectorial transport of the two substrates was absent in the presence of GF120918 (an inhibitor of both P-gp and BCRP) as well (Figure 7A). In the absence of the inhibitors, the apparent permeability coefficient (P_{app}) for the apical-to-basal ($P_{app,A \rightarrow B}$) and basal-to-apical directions ($P_{app,B \rightarrow A}$) of [¹⁴C]esaxerenone at 1 μM was 16.8×10^{-6} and 43.5×10^{-6} cm/s, respectively (Figure 7B), and the P_{app} ratio ($P_{app,B \rightarrow A} / P_{app,A \rightarrow B}$) was calculated as 2.59. Verapamil, novobiocin, and GF120918 affected the permeability of [¹⁴C]esaxerenone (Figure 7B). These results suggested that esaxerenone was a substrate of both P-gp and BCRP. The low P_{app} of mannitol, a low permeability marker drug, suggested the integrity of the Caco-2 cell monolayers during the study (Figure 7B). Theophylline, of which 100% of the dose is absorbed in humans (Li *et al.*, 2007), was evaluated as a highly membrane-permeable marker, and its $P_{app,A \rightarrow B}$ was 22.4×10^{-6} cm/s (Figure 7B).

Metabolism and Excretion of Esaxerenone Hydrolysate in Rats

¹⁴C-Labeled 4-(methylsulfonyl)aniline ([¹⁴C]4MSA), a metabolite generated by the hydrolysis of esaxerenone, was synthesized and administered to F344 rats to investigate the fate of the metabolite. After intravenous administration, the $t_{1/2}$ of the radioactivity in blood and plasma was 6.6 and 6.5 h, respectively. By 24 h after a single intravenous administration, 73.6% and 6.5% of the dosed radioactivity was excreted in urine and feces, respectively. By 96 h after a single intravenous administration, 83.8% and 9.1% of the dosed radioactivity was excreted in the urine and feces, respectively, giving a total excretion of 92.9%. In the metabolite analysis of rat plasma, the acetylated form of 4MSA was mainly observed, and the hydroxylated form of the acetylated 4MSA was also identified. The detailed results are shown in the supplemental data (Supplemental Figure 3).

DMD#84897

Discussion

In this study, [^{14}C]esaxerenone was administered orally to six healthy male volunteers. The maximum dose of esaxerenone administered in a Phase 3 study was 5 mg (<https://clinicaltrials.gov/ct2/show/NCT02890173>); however, 20 mg was administered in this study to ensure the feasibility of metabolite detection. The safety and dose proportionality after single doses of between 5 and 200 mg esaxerenone were confirmed in a Phase 1 study (Kato *et al.*, 2018); therefore, ADME profiles following administration of 20 mg were considered to be comparable with those following administration of 5 mg. Following oral administration, more than 90% of the dosed radioactivity was recovered in urine and feces by 288 h post dose. The half-lives of the radioactivity in blood and plasma were similar to that of the unchanged form, and the value obtained by dividing blood AUC_{last} by plasma AUC_{last} was 0.628, suggesting low partitioning of esaxerenone and its major metabolites into blood components.

The fecal excretion of the unchanged esaxerenone was 18.7%. Assuming that all metabolism occurs after absorption, the absorption ratio (F_a) was considered to be at least 80%. Some drugs are metabolized by intestinal microbiota; however, this is unlikely for esaxerenone because the major metabolites observed in feces were oxidized forms. In monkeys, *O*-glucuronide (M4), a major metabolite in bile, was not detected in feces, suggesting that the glucuronide was hydrolyzed back to the unchanged form by the intestinal flora (Yamada *et al.*, 2017). Because a similar phenomenon is likely to occur in humans, F_a was expected to be over 80%, and a high bioavailability, similar to rats (ca. 100%) and monkeys (ca. 70%), was expected. The high F_a of esaxerenone was also suggested by the experiments using a Caco-2 cell monolayer (Figure 7). When P-gp and BCRP inhibitors were added, the membrane permeability of esaxerenone was similar to that of theophylline, the F_a of which is 100% of the dose in humans (Li *et al.*, 2007). Given the high F_a , the DDI risk of esaxerenone and P-gp/BCRP inhibitors was expected to be low, although in vitro experiments indicated that esaxerenone was a substrate for these transporters.

The low excretion ratio of unchanged form in urine and feces suggested that esaxerenone was mainly cleared

DMD#84897

by metabolism. Metabolite profiling detected several oxidized forms, *O*-glucuronide, and glucuronides of amide-bond hydrolysate, which suggested esaxerenone has multiple metabolic pathways: oxidation, glucuronidation, and hydrolysis. To estimate the contribution of oxidative metabolism, the excretion ratio of the oxidized metabolites (M2, M3, M5, M16, and M17), and the metabolites for which the initial reaction is oxidation (M8 and M13) was summed. Approximately 30% of total body clearance (CL_T) was considered to result from oxidation. Among the oxidized metabolites, production of M1, M2, and M3 with CYP3A4 and CYP3A5 was confirmed in in vitro studies (Figure 5A and Supplemental Figure 2). However, even assuming that esaxerenone was completely oxidized only by CYP3A, the decrease in CL_T by a strong CYP3A inhibitor was estimated to be approximately 30%. In contrast, eplerenone, a marketed MR blocker, is mostly metabolized by CYP3A, and the strong CYP3A inhibitor ketoconazole and the moderate inhibitors erythromycin and fluconazole increased its AUC by 5.39, 2.87, and 2.24 times, respectively (Cook *et al.*, 2004). For this reason, eplerenone is contraindicated with strong CYP3A inhibitors; and dose reduction is required when used concomitantly with moderate CYP3A inhibitors, as written in the INSPRA product label (https://www.accessdata.fda.gov/drugsatfda_docs/label/2002/214371bl.pdf). Esaxerenone is less susceptible to interactions with CYP3A inhibitor than eplerenone, making it favorable as a drug for the treatment of chronic diseases such as hypertension and diabetes.

M11 and M12 were glucuronides of amide-bond hydrolysate of esaxerenone. Further in vitro studies indicated that the hydrolysis occurred independent of NADPH in human liver microsomes, and did not occur in human plasma and liver cytosols (data not shown). The hydrolysis in human liver microsomes was inhibited by several esterase inhibitors: bis-p-nitrophenyl phosphate, phenylmethylsulfonyl fluoride, eserine, diisopropylfluoro phosphate, and p-chloromercuribenzoate (data not shown). The involved enzyme is still unknown, however, the possibility of interaction via hydrolysis was low because the sum of the excretion ratio of M11 and M12 was approximately 13%. The calculation of the contribution of *O*-glucuronic acid is difficult because *O*-glucuronide (M4) is returned to the unchanged form in the intestinal lumen after biliary excretion.

DMD#84897

Nevertheless, the DDI risk via UGT was considered to be low, as multiple UGT isoforms were involved in the glucuronidation of esaxerenone (Figure 6B), and the complete inhibition of all isoforms is unlikely. Multiple UGT isoforms were also involved in the glucuronidation of HMCA, a hydrolyzed form of esaxerenone (data not shown). The formation of M15, a sulfonic acid form, can be explained by initial oxidative demethylation of the methylsulfonyl moiety to generate a sulfinic acid intermediate, followed by oxidative conversion to sulfonic acid. This unusual metabolic pathway from methyl sulfone to sulfonic acid has been reported previously for odanacatib (Kassahun *et al.*, 2011).

The urinary excretion of the unchanged esaxerenone in human was as low as 1.6%, suggesting the low contribution of renal clearance to the CL_t of esaxerenone. Therefore, the DDI potential via inhibition of renal transporters, such as organic anion transporters, organic cation transporters, and multidrug and toxin extrusion transporters, is considered to be low. Furthermore, low urinary excretion suggested that the plasma exposure of esaxerenone was not affected by renal dysfunction. This property was preferable as esaxerenone is expected to be administered to patients with renal impairment, such as hypertension, chronic kidney disease, and type 2 diabetes with microalbuminuria.

Quantification of circulating metabolites is necessary to evaluate their potential toxicity risk. The results of the radio-HPLC analysis showed that unchanged esaxerenone was the major component in plasma, and that the *O*-glucuronide of esaxerenone (M4) and the acyl-glucuronide of amide-bond hydrolysate (M11) were detected as circulating metabolites. The metabolite/radioactivity AUC ratio (AUCR) of M4 was slightly high (21.4%); however, according to the MIST guidance, conjugated metabolites such as *O*-glucuronide are usually less pharmacologically active, so no additional evaluation is required (FDA, 2016). Furthermore, M4 was also a major metabolite in monkey plasma (Yamada *et al.*, 2017), and its concentration in the toxicity study was considered to be higher than that in humans (data not shown). Although the deshydroxyethyl form (M1) was not observed on the radiochromatogram, its plasma concentration was measured by LC-MS/MS because it showed a weak antagonistic effect on MR and its half-life was much longer than that of unchanged form in

DMD#84897

non-clinical studies (data not shown). As predicted, M1 was eliminated very slowly from human plasma; therefore, its AUCR (1.7%) was calculated by using AUC_{last} instead of AUC_{inf} . Owing to its long $t_{1/2}$, the steady-state AUCR of M1 was undetermined; however, it was considered to be less than 10% of total radioactivity exposure as the metabolite-to-parent trough concentration ratio was less than 10% at steady state after 6 weeks' administration of esaxerenone to hypertension patients (data on file).

The AUCR of M11 was not very high (8.0%). Although M11 was not detected in rat and monkey plasma in a previous study (Yamada *et al.*, 2017), it was detected in the toxicity study samples (100 mg/kg for rats and 1000 mg/kg for monkeys) by quantitative LC-MS/MS analysis. The AUC of M11 in rat and monkey plasma was approximately half of that observed in human plasma in the current study (data on file). Considering the dosing amount in the current study was higher than the clinical dose, the exposures in animals are suggested to support those in humans.

The existence of M11 and M12 suggests the exposure of the complementary part, 4MSA, in the human body; however, 4MSA and its metabolites were not detected on the radiochromatogram as this moiety was not radiolabeled. As the hydrolyzed metabolite was not observed in rats and monkeys, further non-clinical evaluation is difficult, even if another [^{14}C]esaxerenone with labeled 4MSA was synthesized. Therefore, [^{14}C]4MSA was synthesized and administered intravenously to rats to investigate its fate. The results indicated that 4MSA was metabolized to the acetylated form, and the radioactivity was excreted mainly into urine (Supplemental Figure 2). The $t_{1/2}$ of the radioactivity after the administration of [^{14}C]4MSA was approximately 6.5 h and similar to that of esaxerenone administered to rats (Yamada *et al.*, 2017), suggesting a low possibility of accumulation of 4MSA and its metabolites. Furthermore, when the concentrations of 4MSA and its metabolites were measured in plasma from healthy volunteers after administration of 5 mg esaxerenone for 14 days, their AUC was less than 3% of that of the unchanged esaxerenone (data not shown).

In conclusion, because of the high absorption ratio and various metabolic pathways involved, the DDI potential of esaxerenone with enzyme inhibitors was considered to be limited. The low urinary excretion of

DMD#84897

unchanged esaxerenone suggested that contribution of renal clearance was limited and that renal impairment did not significantly affect esaxerenone exposure. The exposure of the metabolites of esaxerenone in human plasma was evaluated and was confirmed that they were covered with non-clinical toxicity studies. These characteristics are considered to demonstrate its favorability for clinical use.

Acknowledgments

The authors thank Worldwide Clinical Trials for conducting the clinical study, Celerion for conducting the bioanalysis, and LSI Medience Corporation for conducting the metabolite analysis. The authors also thank Drs. M. Honzumi, Y. Asoh, H. Tsuruoka, and K. Aoki from Daiichi Sankyo for the preparation of authentic standard of the metabolites, and Dr. M. Kotsuma from Daiichi Sankyo Pharma Development for his kind support.

Authorship Contributions

Participated in research design: Yamada, Mendell, Takakusa, Shimizu

Conducted experiments: Yamada, Takakusa

Performed data analysis: Yamada, Mendell, Takakusa

Wrote or contributed to the writing of the manuscript: Yamada, Takakusa, Mendell, Shimizu, Ando

References

- Aoki K, Tsuruoka H, Hayashi N, Yoshida J, and Asoh Y (2008) Atropisomer of pyrrole derivative. International Publication No. WO2008126831A1.
- Arai K, Homma T, Morikawa Y, Ubukata N, Tsuruoka H, Aoki K, Ishikawa H, Mizuno M, and Sada T (2015) Pharmacological profile of CS-3150, a novel, highly potent and selective non-steroidal mineralocorticoid receptor antagonist. *Eur J Pharmacol* **761**:226–234.

DMD#84897

- Arai K, Morikawa Y, Ubukata N, Tsuruoka H, and Homma T (2016) CS-3150, a novel nonsteroidal mineralocorticoid receptor antagonist, shows preventive and therapeutic effects on renal injury in deoxycorticosterone acetate/salt-induced hypertensive rats. *J Pharmacol Exp Ther* **358**:548–557.
- Arai K, Tsuruoka H, and Homma T (2015) CS-3150, a novel non-steroidal mineralocorticoid receptor antagonist, prevents hypertension and cardiorenal injury in Dahl salt-sensitive hypertensive rats. *Eur J Pharmacol* **769**:266–273.
- Brem AS, Morris DJ, and Gong R (2011) Aldosterone-induced fibrosis in the kidney: questions and controversies. *Am J Kidney Dis* **58**:471–479.
- Canne Bannen L, Chen J, Dalrymple, Lisa E, Flatt, Breton T, Forsyth, Timothy, Patrick Gu X-H, Mac, Morrison B, Mann, Larry W, Mann G, Martin R, Mohan R, Murphy B, Nyman, Michael C, Stevens, William, C. J, Wang T-L, Wong Y, and Wu, Jason H (2006) Pyrrole derivatives as pharmaceutical agents. International Publication No. WO2006012642A2.
- Cook CS, Berry LM, and Burton E (2004) Prediction of in vivo drug interactions with eplerenone in man from in vitro metabolic inhibition data. *Xenobiotica* **34**:215–228.
- Epstein M, Williams GH, Weinberger M, Lewin A, Krause S, Mukherjee R, Patni R, and Beckerman B (2006) Selective aldosterone blockade with eplerenone reduces albuminuria in patients with type 2 diabetes. *Clin J Am Soc Nephrol* **1**:940–951.
- FDA (2016) Guidance for Industry: Safety Testing of Drug Metabolites, US Department of Health and Human Services FaDA, Center for Drug Evaluation and Research.
- Funder JW (1996) Mineralocorticoid Receptors and Hypertension. *J Steroid Biochem Mol Biol* **53**:53–55.
- Kassahun K, Black WC, Nicoll-Griffith D, McIntosh I, Chauret N, Day S, Rosenberg E, and Koeplinger K (2011) Pharmacokinetics and metabolism in rats, dogs, and monkeys of the cathepsin k inhibitor odanacatib: Demethylation of a methylsulfonyl moiety as a major metabolic pathway. *Drug Metab Dispos* **39**:1079–1087.
- Kato M, Furuie H, Shimizu T, Miyazaki A, Kobayashi F, and Ishizuka H (2018) Single - and multiple - dose

DMD#84897

- escalation study to assess pharmacokinetics, pharmacodynamics, and safety of oral esaxerenone in healthy Japanese subjects. *Br J Clin Pharmacol* **84**:1821–1829, in press.
- Lombès M, Alfaidy N, Eugene E, Lessana A, Farman N, and Bonvalet J-P (1995) Prerequisite for cardiac aldosterone action: mineralocorticoid receptor and 11 β -hydroxysteroid dehydrogenase in the human heart. *Circulation* **92**:175–182.
- Nagai Y, Miyata K, Sun G-P, Rahman M, Kimura S, Miyatake A, Kiyomoto H, Kohno M, Abe Y, Yoshizumi M, and Nishiyama A (2005) Aldosterone stimulates collagen gene expression and synthesis via activation of ERK1/2 in rat renal fibroblasts. *Hypertension* **46**:1039–1045.
- Nishiyama A, Yao L, Fan Y, Kyaw M, Kataoka N, Hashimoto K, Nagai Y, Nakamura E, Yoshizumi M, Shokoji T, Kimura S, Kiyomoto H, Tsujioka K, Kohno M, Tamaki T, Kajiya F, and Abe Y (2005) Involvement of aldosterone and mineralocorticoid receptors in rat mesangial cell proliferation and deformability. *Hypertension* **45**:710–716.
- Patni H, Mathew JT, Luan L, Franki N, Chander PN, and Singhal PC (2007) Aldosterone promotes proximal tubular cell apoptosis: role of oxidative stress. *Am J Physiol Physiol* **293**:F1065–F1071.
- Pitt B, Remme W, Zannad F, Neaton J, Martinez F, Roniker B, Bittman R, Hurley S, Kleiman J, and Gatlin M (2003) Eplerenone, a selective aldosterone blocker, in patients with left ventricular dysfunction after myocardial infarction. *N Engl J Med* **348**:1309–1321.
- Pitt B, Zannad F, Remme WJ, Cody R, Castaigne A, Perez A, Palensky J, and Wittes J (1999) The effect of spironolactone on morbidity and mortality in patients with severe heart failure. *N Engl J Med* **341**:709–717.
- Rautio J, Humphreys JE, Webster LO, Balakrishnan A, Keogh JP, Kunta JR, Serabjit-Singh CJ, and Polli JW (2006) In vitro P-glycoprotein inhibition assays for assessment of clinical drug interaction potential of new drug candidates: A recommendation for probe substrates. *Drug Metab Dispos* **34**:786–792.
- Rose LI, Underwood RH, Newmark SR, Kisch ES, and Williams GH (1977) Pathophysiology of spironolactone-induced gynecomastia. *Ann Intern Med* **87**:398–403.

DMD#84897

Rossing K, Schjoedt KJ, Smidt UM, Boomsma F, and Parving HH (2005) Beneficial effects of adding spironolactone to recommended antihypertensive treatment in diabetic nephropathy: A randomized, double-masked, cross-over study. *Diabetes Care* **28**:2106–2112.

Saruta T, Kageyama S, Ogihara T, Hiwada K, Ogawa M, Tawara K, Gatlin M, Garthwaite S, Bittman R, and Patrick J (2004) Efficacy and safety of the selective aldosterone blocker eplerenone in Japanese patients with hypertension: a randomized, double-blind, placebo-controlled, dose-ranging study. *J Clin Hypertens* **6**:175–183.

Shibata S, Nagase M, Yoshida S, Kawachi H, and Fujita T (2007) Podocyte as the target for aldosterone: roles of oxidative stress and Sgk1. *Hypertension* **49**:355–364.

Siragy HM, and Xue C (2008) Local renal aldosterone production induces inflammation and matrix formation in kidneys of diabetic rats. *Exp Physiol* **93**:817–824.

Weinberger MH, Roniker B, Krause SL, and Weiss RJ (2002) Eplerenone, a selective aldosterone blocker, in mild-to-moderate hypertension. *Am J Hypertens* **15**:709–716.

Xia CQ, Yang JJ, and Gan LS (2005) Breast cancer resistance protein in pharmacokinetics and drug-drug interactions. *Expert Opin Drug Metab Toxicol* **1**:595–611.

Yamada M, Takei M, Suzuki E, Takakusa H, Kotsuma M, Washio T, Murayama N, Inoue S, and Izumi T (2017) Pharmacokinetics, distribution, and disposition of esaxerenone, a novel, highly potent and selective non-steroidal mineralocorticoid receptor antagonist, in rats and monkeys. *Xenobiotica* **47**:1090–1103.

DMD#84897

Legends for Figures

Figure 1 Chemical structures of [^{14}C]esaxerenone (A) and deuterium-labeled-esaxerenone (B)

Figure 2 Mean concentrations of radioactivity in blood and plasma (A), and esaxerenone and its metabolites M1, M4, and M11 in plasma (B) following a single oral administration of [^{14}C]esaxerenone. Each point represents the mean \pm SD of six subjects.

Figure 3 Mean cumulative excretion of total radioactivity in urine and feces following a single oral administration of [^{14}C]esaxerenone. Each point represents the mean \pm SD of six subjects.

Figure 4 Representative radiochromatograms of the metabolites in human plasma (1 h), urine (0–24 h), and feces (24–48 h) following oral administration of [^{14}C]esaxerenone at a dose of 20 mg.

Figure 5 Proposed major metabolic pathway of esaxerenone in humans. The structures of M1, M2, M3, M4, M5, and M11 were validated against authentic standards. The structures of other metabolites were proposed based on MS/MS fragmentation and consistency with the validated metabolite structures. Some metabolites of which structures have not been identified are not included.

Figure 6 Formation rates of the metabolites from esaxerenone in microsomes expressing human P450 isoforms (A) and UGT isoforms (B). Control (KPB) indicates control microsomes in potassium phosphate buffer and Control (Tris) indicates control microsomes in Tris buffer. ND indicates not detected.

Figure 7 Transcellular transport across Caco-2 cell monolayers and the effect of verapamil (VPM, P-gp inhibitor), novobiocin (NVB, BCRP inhibitor), and GF120918 (GF, P-gp and BCRP inhibitor) of digoxin and estrone sulfate (A); esaxerenone, theophylline (TPL), and mannitol (MAN) (B). A

DMD#84897

minus sign indicates no inhibitor.

DMD#84897

Tables

Table 1 Pharmacokinetic parameters of radioactivity in blood and plasma, and esaxerenone and its metabolites in plasma after a single oral administration of [¹⁴C]esaxerenone to healthy volunteers.

Parameter	Unit	¹⁴ C Plasma	¹⁴ C Blood
C _{max}	ng-eq./mL	430 (65)	281 (39)
AUC _{last}	ng-eq.·h/mL	12600 (2100)	7880 (1210)
AUC _{inf}	ng-eq.·h/mL	12900 (2100)	8180 (1240)
t _{1/2}	h	30.8 (3.9)	29.6 (4.9)
T _{max}	h	3.75 (2.00, 6.02)	3.25 (2.00, 6.02)
Blood-to-plasma AUC _{last} ratio		0.628 (0.014)	

Parameter	Unit	Esaxerenone	M4	M11	M1
C _{max}	ng/mL	237 (60)	165 (40)	39.0 (2.9)	1.00 (0.30)
AUC _{last}	ng·h/mL	5310 (1390)	3860 (1190)	1060 (70)	198 (57)
AUC _{inf}	ng·h/mL	5320 (1390)	3860 (1190)	1070 (70)	NC
t _{1/2}	h	34.0 (9.8)	27.8 (12.9)	26.4 (10.2)	NC
T _{max}	h	2.25 (1.50, 4.00)	4.00 (2.00, 6.02)	3.75 (3.00, 6.02)	48.0 (48.0, 96.0)
CL/F	L/h	3.96 (0.94)	NC	NC	NC
V _z /F	L	187 (36)	NC	NC	NC
AUCR ^a	%	40.8 (5.7)	21.4 (4.2)	8.0 (0.8)	1.7 (0.6)

^a Metabolite/¹⁴C plasma AUC_{inf} ratio corrected for molecular weight. AUC_{last} was used for M1.

Arithmetic means (standard deviations) of six subjects, with the exception of T_{max}, for which the medians (minimum, maximum) are shown.

DMD#84897

Table 2 Mass spectral analysis of esaxerenone metabolites detected in human plasma, urine, and feces

Metabolite		[M-H] ⁻	Elemental	Characteristic fragment
No.	Biotransformation	(<i>m/z</i>)	composition	ions (<i>m/z</i>)
Esaxerenone		465	C ₂₂ H ₂₁ F ₃ N ₂ O ₄ S	365, 224, 170
M1	Deshydroxyethyl form	421	C ₂₀ H ₁₇ F ₃ N ₂ O ₃ S	224, 184, 170
M2	Carboxylic acid form	479	C ₂₂ H ₁₉ F ₃ N ₂ O ₅ S	365, 170
M3	Oxygenation	481	C ₂₂ H ₂₁ F ₃ N ₂ O ₅ S	419, 381, 363, 351, 170
M4	O-Glucuronide	641	C ₂₈ H ₂₉ F ₃ N ₂ O ₁₀ S	465, 447, 365, 224, 170
M5	Hydroxymethyl-carboxylic acid form	495	C ₂₂ H ₁₉ F ₃ N ₂ O ₆ S	381, 363, 351, 196, 170
M8	Glucuronide of monooxygenated form	657	C ₂₈ H ₂₉ F ₃ N ₂ O ₁₁ S	481, 419, 381, 170
M11	Acyl-glucuronide of amide-bond hydrolysate	488	C ₂₁ H ₂₂ F ₃ NO ₉	312, 268, 238, 175
M12	O-Glucuronide of amide-bond hydrolysate	488	C ₂₁ H ₂₂ F ₃ NO ₉	312, 294, 268
M13	Glucuronide of monooxygenated form	657	C ₂₈ H ₂₉ F ₃ N ₂ O ₁₁ S	481, 419, 363, 170
M15	Sulfonic acid form	467	C ₂₁ H ₁₉ F ₃ N ₂ O ₅ S	343, 287, 198, 172
M16	Dioxygenated form	497	C ₂₂ H ₂₁ F ₃ N ₂ O ₆ S	not detected
M17	Dioxygenated form	497	C ₂₂ H ₂₁ F ₃ N ₂ O ₆ S	351, 300, 170

DMD#84897

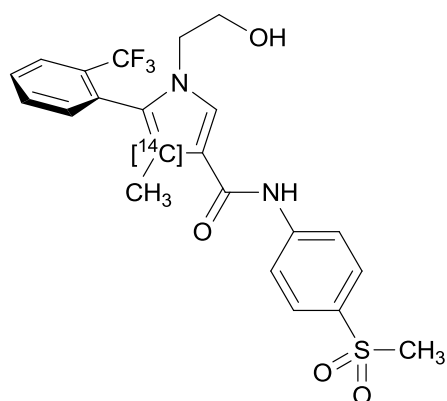
Table 3 Excretion of esaxerenone and its metabolites in urine and feces after oral administration of [¹⁴C]esaxerenone

Metabolite No.	Identification	Excretion ratio (% of dose)	
		Urine	Feces
		0 to 72 h	0 to 168 h
-	Esaxerenone	1.6	18.7
M2	Carboxylic acid form	2.6	9.0
M3+M5	Hydroxymethyl form + Hydroxymethyl-carboxylic acid form	1.7	10.1
M4	O-Glucuronide	7.2	-
M8	Glucuronide of monooxygenated form	1.6	-
M11	Glucuronide of amide-bond hydrolysate	10.5	-
M12	O-Glucuronide of amide-bond hydrolysate	2.5	-
M13	Glucuronide of monooxygenated form	1.3	-
M15	Sulfonic acid form	-	0.9
M16	Dioxygenated form	-	1.6
M17	Dioxygenated form	-	1.0
Others	(Sum of other unknown small peaks)	4.8	9.8
Total radioactivity		33.8	51.0

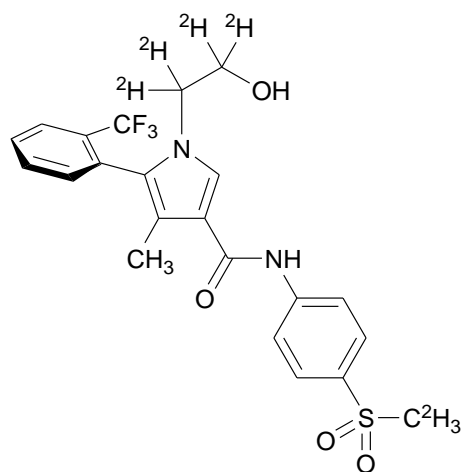
DMD#84897

Figure 1

(A)

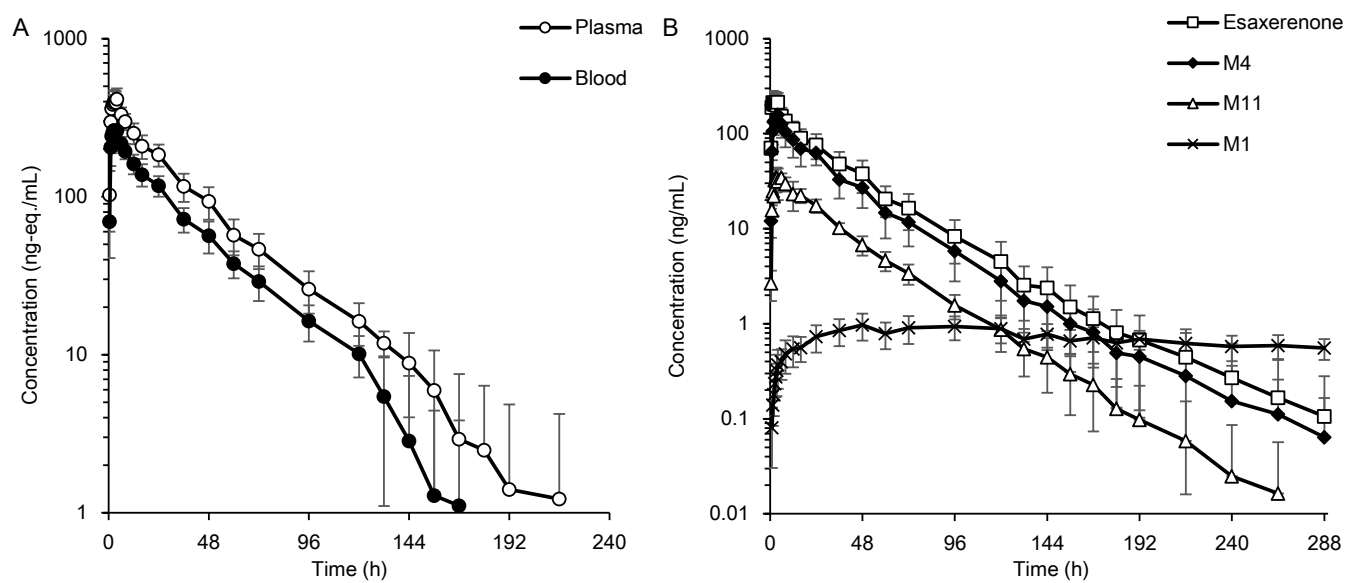


(B)



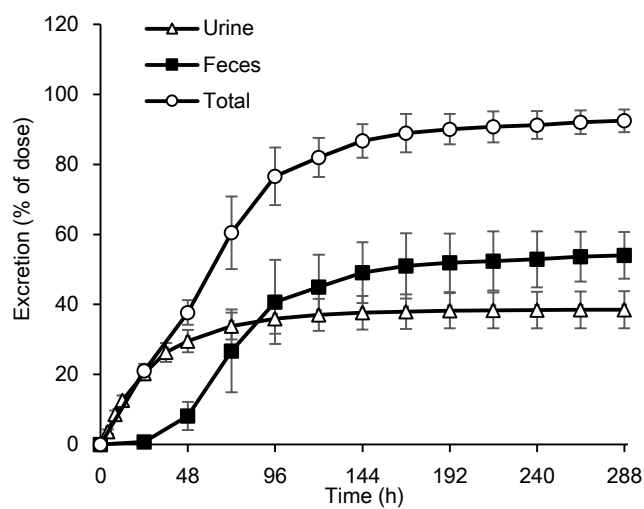
DMD#84897

Figure 2



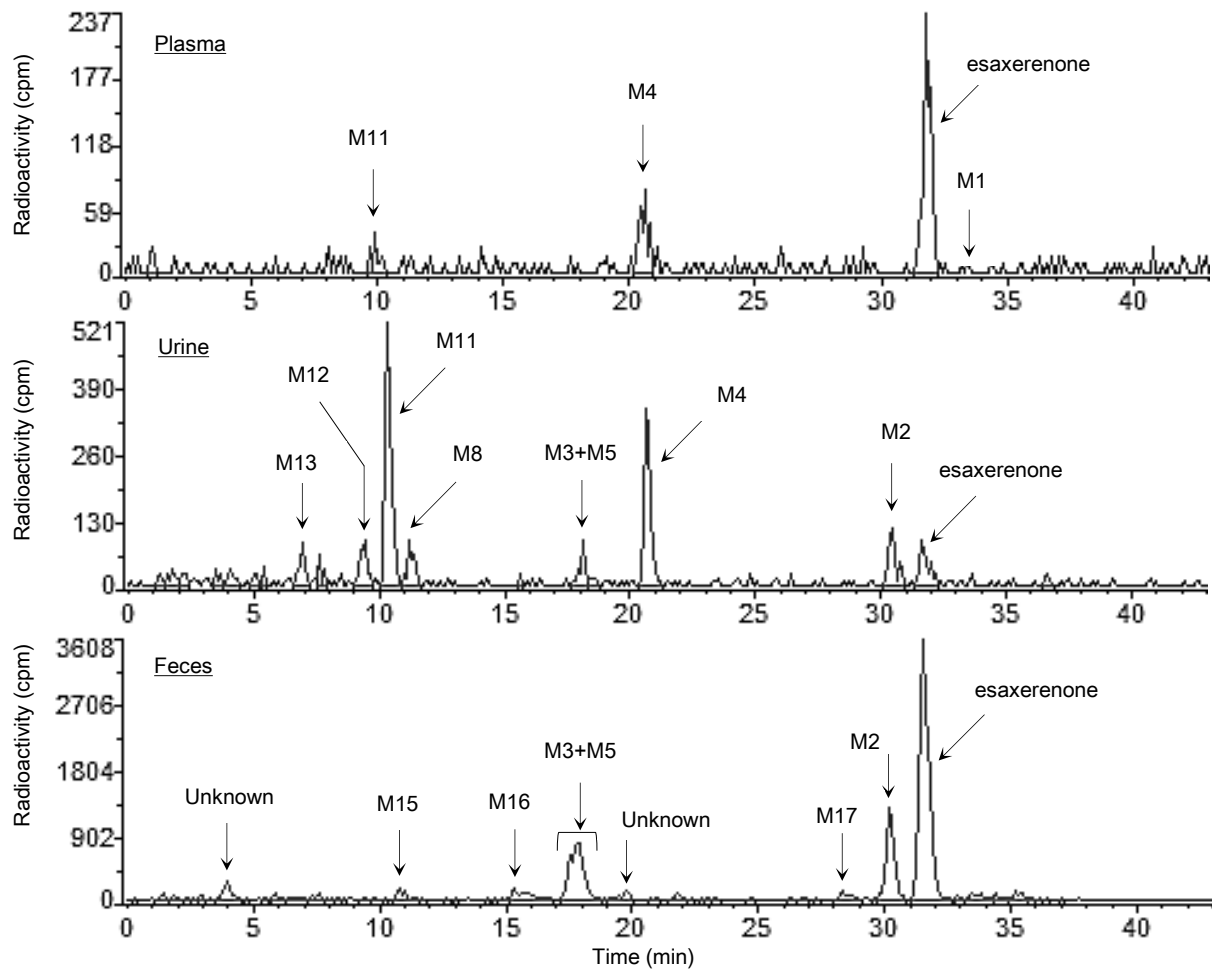
DMD#84897

Figure 3



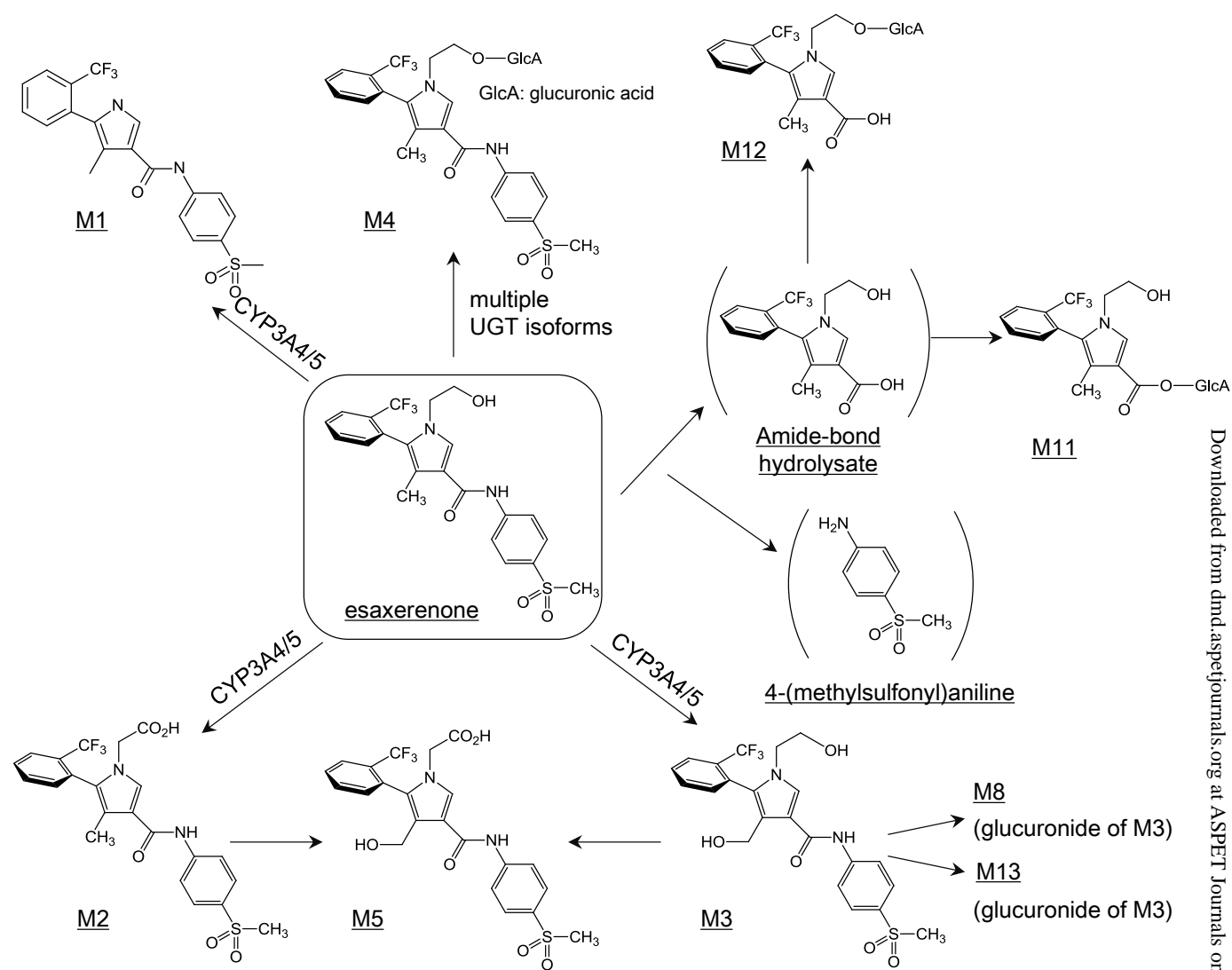
DMD#84897

Figure 4



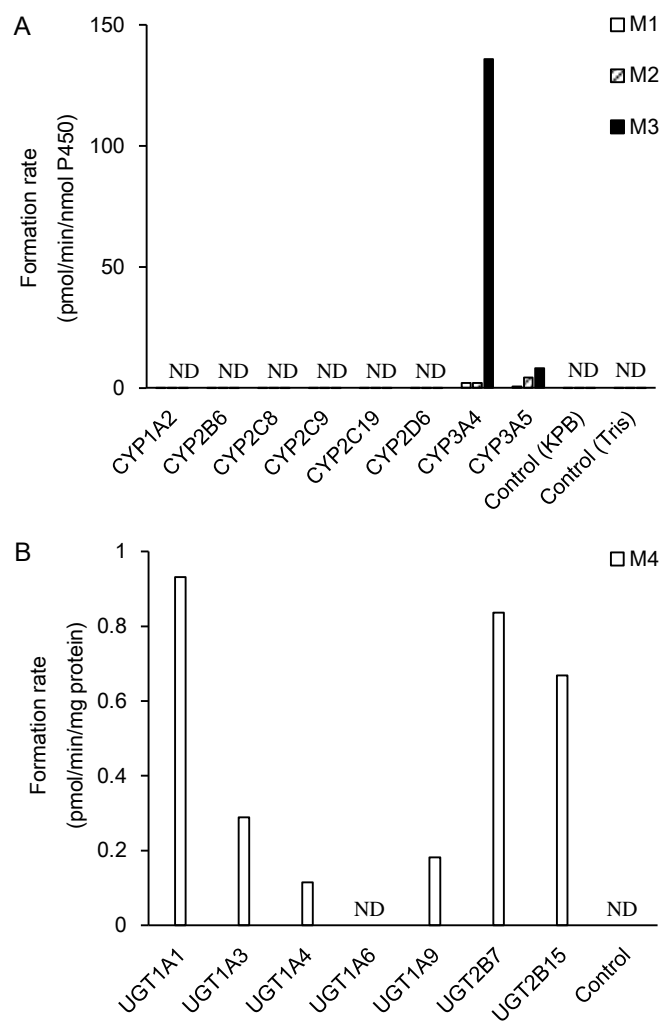
DMD#84897

Figure 5



DMD#84897

Figure 6



DMD#84897

Figure 7

